# A Kinetic Description of Diffusion-Controlled Intramolecular Excimer Formation and Dissociation. 2. An Interpretation of the Birks Scheme and Treatment of Experimental Data

**Guojun Liu**

*Department of Chemistry, The University of Calgary, 2500 University Drive, NW, Calgary, Alberta, Canada T2N 1N4*

*Received August 27, 1991; Revised Manuscript Received May 1, 1992*

ABSTRACT: Transient intensity profiles of monomer and excimer emission are computed numerically using equations derived from the new approach proposed by Liu and Guillet for the description of the kinetics of excimer formation and dissociation involving chromophores attached to the opposite ends of a polymer chain. The profiles generated are fitted with expressions for the transient monomer and excimer intensities derived from the Birks scheme. The validity of these equations of the Birks scheme in approximating these profiles is judged from the goodness of fitting and the appropriateness of the fitting parameters generated. The Birks scheme is shown to be valid only under limited circumstances, and the criterion for the validity is established. The significance of the rate constants of the Birks scheme and factors which affect the magnitude of them are discussed in terms of the Liu and Guillet model. Finally, the transient monomer and excimer intensity profiles, monitored by Winnik et al. experimentally, for pyrene groups attached to the opposite ends of polystyrene chains of different molecular weights are fitted using equations of the Liu and Guillet theory to yield the coefficient of relative diffusion, $D$, between polystyrene chain ends. The values of $D$ are compared with those calculated from rate constants $k_1$ and equations of the Wilemski–Fixman theory.

## I. Introduction

The rate of diffusion-controlled intramolecular excimer formation from chromophores attached to opposite ends of a polymer chain after excitation of one of the end groups by pulse radiation depends on two factors. First, it depends on how the end groups M are distributed at the time of pulse excitation. If they are close to one another, slight adjustment of conformations of the connecting chain due to segmental rotation can lead to the formation of an excimer. If the end groups are separated by a large distance at $t = 0$, large-scale segmental motion of the chain is required to bring the end groups close to form an excimer. Thus, excimer formation is slower in the latter case than in the former case. Then, the rate of excimer formation depends on how fast the end groups move relative to one another. If a phenomenological diffusion coefficient, $D$, can be used to describe the relative motion of the ends of a polymer chain, a larger $D$ leads to faster excimer formation. In conclusion, the study of the kinetics of diffusion-controlled excimer formation from M* and M attached to the ends of a polymer chain can provide insight into the statistics, the initial end-to-end distance distribution function, and the dynamics, i.e., the fluctuation of the end-to-end distance with time, of the connecting chain.

Previously, the kinetics for intramolecular excimer formation and dissociation has been described by the Birks scheme[1]

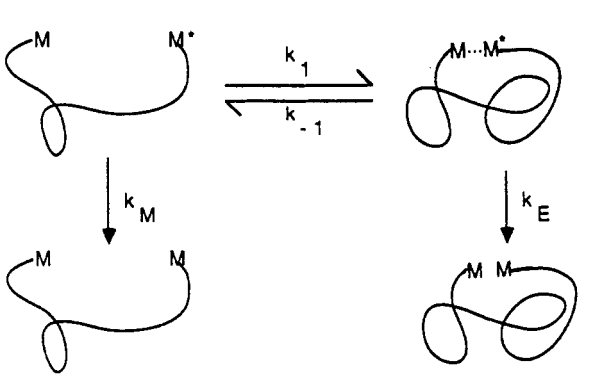


where $k_M$ is the rate constant for the self-deactivation of M* and is equal to the inverse of the fluorescence lifetime, $\tau_M$, of M* in the absence of excimer formation, $k_E$ is the rate constant for the self-deactivation of an excimer M···M* and is equal to $1/\tau_E$, and $k_1$ and $k_{-1}$ are rate constants for excimer formation and dissociation, respectively. If $k_1$ and $k_{-1}$ are uniquely defined, the Birks scheme predicts that the intensity of fluorescence of monomer M* decays as a sum of two exponential terms:[2]

$$I_M(t) = A_1 e^{-\lambda_1 t} + A_2 e^{-\lambda_2 t} \tag{1}$$

where $A_1/A_2$, $\lambda_1$, and $\lambda_2$ are functions of $k_1$, $k_{-1}$, $k_M$, and $k_E$. Under the same conditions, the excimer emission intensity $I_E(t)$ should grow in and decay as the difference of two exponential terms:

$$I_E(t) = A_3 e^{-\lambda_3 t} + A_4 e^{-\lambda_4 t} \tag{2}$$

where

$$A_3 = -A_4 \tag{3a}$$

$$\lambda_3 = \lambda_1 \tag{3b}$$

$$\lambda_4 = \lambda_2 \tag{3c}$$

If the Birks scheme holds, the rate constants $k_1$, $k_{-1}$, and $k_E$ can be calculated from decay parameters recovered using the following equations:[2]

$$\lambda_1,\lambda_2 = (1/2)\{(Y + X) \mp [(Y - X)^2 + 4k_1k_{-1}]^{1/2}\} \tag{4}$$

and

$$A_2/A_1 = (X - \lambda_1)/(\lambda_2 - X) \tag{5}$$

where

$$X = k_M + k_1 \tag{6}$$

and

$$Y = k_E + k_{-1} \tag{7}$$

Rate constant $k_1$, obtainable from the Birks scheme, can yield information about the statistics and dynamics of polymer chains. According to Wilemski and Fixman,[3-5]

0024-9297/92/2225-5805$03.00/0 

the diffusion-controlled quenching of the fluorescence of an excited chromophore attached to one end of a chain by a quencher attached to the other end makes the intensity of the fluorescence of the excited chromophore decay as a sum of exponential terms:

$$\chi(t) = \sum_i a_i \exp(-k_i t) \tag{8}$$

where $k_i$ is the $i$th-order quenching rate constant and $a_i$ are the amplitude coefficients. For a polymer chain represented by the harmonic spring model,[6] $k_1$ of the fluorescence quenching reaction is related to the root-mean-square end-to-end distance $R_n$ of the chain and the relative diffusion coefficient $D$ of the chain ends by[7-9]

$$k_1 = (6/\pi^{1/2})DR_e/R_n^3, \quad \text{for } R_e/R_n \to 0 \tag{9}$$

where $R_e$, the effective radius for the quenching reaction, denotes the separation distance at which the quenching reaction between an excited chromophore and a quencher group takes place instantaneously. From eq 9, the knowledge of $k_1$ can thus lead to either $R_n$ or $D$.

Fluorescence quenching rate constant $k_1$ is equal to $k_1$ of the Birks scheme for excimer formation due to the similarity between the two processes. In both cases, a short-lived light pulse is used to excite one of the end groups and then the formation of an excimer or the quenching of the fluorescence occurs at a diffusion-controlled rate. In the fluorescence quenching case, fluorescence of the excited end group is quenched by a group of a different kind attached to the other end, and the process is usually irreversible. In the case of excimer formation, fluorescence of excited monomers is quenched due to excimer formation. The fundamental difference between the two processes lies in the reversibility. Excimer formation is reversible and the kinetic scheme for describing the process is more complicated. As far as the forward reactions, excimer formation and fluorescence quenching, are concerned, similar factors, the diffusivity of the chain ends and the initial distribution of the end groups, determine the magnitude of $k_1$.

The disadvantage of the Birks scheme is that it is valid only if the excimer formation process can be approximately described by a single rate constant. That is, $k_1 \ll k_2 < k_3$ in eq 8. This condition may not be satisfied all the time. In cases when a single rate constant is insufficient to describe the excimer formation process, more than one exponential term is needed to describe the decay in monomer intensity due to excimer formation. The kinetics of excimer formation and dissociation thus becomes very complex.

The sum of a few or more exponentially decaying terms can be approximated by a single exponential term with a rate constant $k_1(t)$ which is time-dependent;[8] i.e., $k_1(t)$ is large when $t$ is small and approaches a constant, i.e., $k_1$, as $t \to \infty$. This makes the kinetics simpler, but the final expressions for $I_D(t)$ and $I_M(t)$ are still far more complex than those given by eqs 1 and 2.[10-12] Furthermore, the use of a time-dependent rate constant contradicts the conventional definition of a rate constant, and no one has so far discussed the likely dependence of $k_{-1}$ on $t$. In summary, the particular case of excimer formation needs specific consideration from a statistical mechanical point of view.

Liu and Guillet have recently proposed a statistical theory specifically for the treatment of the kinetics of excimer formation and dissociation.[13] The theory made no use of rate constants $k_1$ and $k_{-1}$ for the description of excimer formation and dissociation. Instead, the excimer formation and dissociation processes are identified with the coming together and diffusing apart of the ends under the action of an excimer interaction potential. The theory has been shown to generate reasonable monomer and excimer transient intensity profiles. In this paper, the theory will be subjected to further scrutinizing by seeing whether it can be used to account for the applicability of the Birks scheme in describing intramolecular excimer formation kinetics in certain cases and to generate reasonable parameters from treating experimentally observed data. In section II, the Liu–Guillet (L–G) theory will be outlined. Section III describes the computational techniques employed. Section IV discusses the equivalence of the L–G theory and the Birks scheme under certain conditions and the breakdown of the Birks scheme under other conditions. The criteria for the validity of the Birks scheme will be established. In cases when the Birks scheme holds, the effect of various parameters appearing in the L–G theory on the rate constants $k_1$ and $k_{-1}$ will be discussed. In section V, the transient monomer and excimer intensity profiles, monitored by Winnik et al.[1] experimentally, for pyrene groups attached to the opposite ends of polystyrene chains of different molecular weights are fitted using the L–G theory to yield the coefficient of relative diffusion between polymer chain ends. The coefficients are then compared with those calculated from rate constants $k_1$ and equations of the Wilemski–Fixman (W–F) theory.

## II. Outline of the Liu–Guillet Theory

The L–G theory assumes that before the excitation of one of the end groups of a polymer chain the end-to-end distance distribution function of the chain is Gaussian[14]

$$G(R) = \left(\frac{3}{2\pi R_n^2}\right)^{3/2} \exp\left(-\frac{3R^2}{2R_n^2}\right) \tag{10}$$

where $R_n$, the root-mean-square end-to-end distance, is related to the statistical bond length $\beta$ and the number of bonds $N$ in a chain by

$$R_n = (N^{1/2})\beta \tag{11}$$

For a chain of finite length $m_x$, the Gaussian distribution function is normalized so that

$$G'(R) = G(R)/\int_0^{m_x} 4\pi R^2 G(R)\, dR \tag{12}$$

After one of the end groups is excited, an excimer interaction potential $U(R)$ is switched on between the ends. The relative diffusion of the end groups is now governed both by a potential derived from the connecting chain and by the excimer interaction potential. If the excited state, either as M* or M···M*, does not deactivate and enough time is allowed for the system to adjust to the newly switched on excimer interaction potential, the final new equilibrium end-to-end distance distribution function should be[13]

$$P(R) = \alpha G(R) \exp[-U(R)/(k_B T)] \tag{13}$$

where $k_B T$ is the thermal energy; $\alpha$, the normalization factor, is given by

$$\alpha^{-1} = \int_0^{m_x} 4\pi R^2 G(R) \exp[-U(R)/(k_B T)]\, dR \tag{14}$$

The distribution function $P(R)$ is thus derived from the original Gaussian end-to-end distance distribution function modified by a Boltzmann energy weighting factor $\exp[-U(R)/(k_B T)]$.

The excimer interaction potential is assumed to possess the general form

$$U(R) = -\epsilon_0[2(R_0/R)^n - (R_0/R)^m] \quad (15)$$

where $n$ is less than $m$, indicating that the attractive part of the potential is longer-ranged than the repulsive part. For $m = 2n$, $R_0$ is the distance at which $U(R)$ is minimal, and $-\epsilon_0$ is equal to the Gibbs free energy for excimer formation at $R = R_0$. For an arbitrary set of $n$ and $m$ values, the energy minimum occurs at end-to-end separation distances $R_m$, and $R_m$ are related to $R_0$ by

$$R_m = [(m/(2n)]^{1/(m-n)}R_0 \quad (16)$$

The value $\epsilon_0$, in this case, is related to the Gibbs free energy of excimer formation at $R_m$ by

$$U(R_m) = -\epsilon_0[2(2n/m)^{n/(m-n)} - (2n/m)^{m/(m-n)}] \quad (17)$$

The disagreement between $R_m$ and $R_0$ or that between $U(R_m)$ and $-\epsilon_0$ for $m \neq 2n$ should not be of particular concern, because the interaction potential is hypothetically independent of $n$ and $m$. Furthermore, the difference between $R_m$ and $R_0$ and that between $U(R_m)$ and $-\epsilon_0$ are quite small for the frequently used $m$ and $n$ combination, $m = 10$ and $n = 3$, in this paper.

The shift of the system from the first equilibrium state, with end-to-end distance distribution function given by eq 12, to the second equilibrium state, with end-to-end distance distribution function given by eq 13, is usually described by a diffusion-type partial differential equation.[15] The form of the partial differential equation depends on the dynamic model used for describing the chain.[3-5] In a previous paper,[13] the harmonic spring model was used, and the partial differential equation obtained has been found to be difficult to solve analytically. A difference equation approach was thus attempted. The solution of the difference equation leads to the probability $S(R,t+1/\psi)$ for finding chains with end groups separated by a distance $R$ at time $t + 1/\psi$ from $S(R,t)$:

$$S(R,t+1/\psi) = \rho(R+\delta_R \rightarrow R)\, S(R+\delta_R,t) + \rho(R-\delta_R \rightarrow R)\, S(R-\delta_R,t) \quad (18)$$

Since $S(R,t=0)$ is known and is equal to $4\pi R^2G'(R)\delta_R$, eq 18, in principle, can be used to solve for $S(R,t)$ for any subsequent times.

Equation 18 was derived based on a jumping model.[16] In this model, the fluctuation in the end-to-end distance of a polymer chain due to diffusion is visualized as derived from the random jump of one end group in space around the other fixed in the origin of a spherical coordinate system. The jumps occur at high frequency $\psi$. By making each jump, the end-to-end distance is changed by a very small average value $\delta_R$. $\delta_R$ and $\psi$ of the jump model are related to $D$, the relative diffusion coefficient, of the macroscopic diffusion model by the Einstein-Smoluchowski equation[17]

$$D = (1/2)\psi\delta_R^2 \quad (19)$$

The function $\rho(R+\delta_R \rightarrow R)$ of eq 18 denotes the probability for the moving end to make a jump from separation distance $R + \delta_R$ to $R$, and $\rho(R-\delta_R \rightarrow R)$ is that from separation distance $R - \delta_R$ to $R$. $\rho(R \rightarrow R+\delta_R)$ is defined by

$$\rho(R \rightarrow R+\delta_R) = \mathcal{P}(R+\delta_R)/[\mathcal{P}(R+\delta_R) + \mathcal{P}(R-\delta_R)] \quad (20)$$

where $\mathcal{P}(R)$, the equilibrium radial distribution function, is related to $P(R)$, the equilibrium end-to-end distance distribution function of eq 13 by

$$\mathcal{P}(R) = 4\pi R^2P(R) \quad (21)$$

The significance of eq 20 is obvious. If the moving end is $R$ distance away from the other end at time $t$, it will definitely move somewhere else at time $t + 1/\psi$. There are two possible ways for the moving end to make a jump: i.e., either to position $R + \delta_R$ or to position $R - \delta_R$. The probability for it to jump to a position with the end-to-end distance of $R + \delta_R$ should be proportional to the equilibrium probability of finding the end groups separated by that distance. The probability for the end group to make a jump to decrease the end-to-end distance by $\delta_R$ is

$$\rho(R \rightarrow R-\delta_R) = \mathcal{P}(R-\delta_R)/[\mathcal{P}(R+\delta_R) + \mathcal{P}(R-\delta_R)] \quad (22)$$

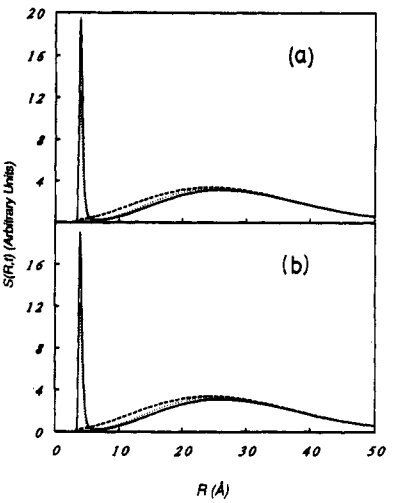


**Figure 1.** Evolution of end-to-end distance distribution function $S(R,t)$ with time after the excitation of one of the end groups of a polymer chain by a $\delta$-pulse at time $t = 0$. Curves (- - -) are the end-to-end distance distribution functions at $t = 1 \times 10^{-3}$ ns, curves (···) are those at $t = 1$ ns, and curves (—) are those at $t = 2$ ns. In (a), neither monomers nor excimers are assumed to deactivate. In (b), monomers are assumed to deactivate with rate constant $4.14 \times 10^6$ s$^{-1}$, and excimers deactivate with rate constant $1.93 \times 10^7$ s$^{-1}$.

A sample solution of eq 18 is shown in Figure 1a. To solve eq 18, the end-to-end distance distribution function at the time of $\delta$-pulse excitation, i.e., $t = 0$, was assumed Gaussian as given by eq 12. The root-mean-square end-to-end distance $R_n$ for the Gaussian chain was assumed to be 30 Å. The coefficient of relative diffusion between the chain ends $D$ was assumed to be $2.0 \times 10^{-6}$ cm$^2$/s. The excimer interaction potential was assumed to possess the form given by eq 15, of which $n = 3$, $m = 10$, $R_0 = 3.6$ Å, and $\epsilon_0 = 8.45k_BT$. As can be seen from Figure 1a, the peak centered around 3.9 Å, close to $R_m$, which is 3.87 Å, increases as time delay after the $\delta$-pulse increases from $1 \times 10^{-3}$ ns, curve (- - -), to 1 ns, curve (···), to 2 ns, curve (—). Excimers are thus formed as a consequence of end-group diffusion, and no rate constants are required for the description of the process as is done in the Birks scheme.

In reality, both excimers and excited monomers deactivate to the ground state, and those deactivation processes need to be taken into account for the correct description of the kinetic behavior of the system. An excimer, according to previous definition,[13] is an M* and M pair which are separated by $R_m$, because the interaction free energy, defined by eq 15, is minimal when M* and M are separated by $R_m$. M* and M are a perfect monomeric pair when they are separated by infinite distances, because at such distances the excimer interaction potential for the

pair is zero. At intermediate end-to-end distances, M* and M are intermediates between a monomeric pair M* + M and an excimer. In addition, chromophores which are separated by distances shorter than $R_m$ are arbitrarily defined as excimers. The arbitrariness is inconsequential because the probability of finding chains with ends separated by distances less than $R_m$ is small. Supposing that M* and M are separated by $R$, the degree of excimer feature is quantified by

$$X(R) = [2(R_0/R)^n - (R_0/R)^m]/[2(R_0/R_m)^n - (R_0/R_m)^m], \quad R \geq R_m \quad (23)$$

because the relative stabilization free energy $U(R)/U(R_m)$ for the pair is equal to $X(R)$. The extent of monomer behavior is then given by $1 - X(R)$.

It is further assumed that a perfect monomer decayed with a self-deactivation rate constant $k_M$ and an excimer with a rate constant $k_E$. An intermediate between an excimer and a monomer decays with rate constant

$$k(R) = k_M[1 - X(R)] + k_E X(R) \quad (24)$$

The diffusion–reaction equation was obtained by incorporating the self-deactivation processes of excimers and monomers into eq 18:

$$S(R,t+1/\psi) = \rho(R+\delta_R \rightarrow R)[1 - k(R+\delta_R)/\psi]S(R+\delta_R,t) + \rho(R-\delta_R \rightarrow R)[1 - k(R-\delta_R)/\psi]S(R-\delta_R,t) \quad (25)$$

Equation 25 is derived from eq 18 by realizing that during the time interval $1/\psi$, the excitation energy of an end group which is $R$ distance away from the other end group at the origin decays following the rate law

$$dS(R,t)/dt = -k(R)\, S(R,t) \quad (26)$$

where $S(R,t)$ is now the joint probability for finding an end group which is distance $R$ away from the other end and excited at time $t$.

A sample solution of eq 25 is shown in Figure 1b. In addition to those parameters used in generating the curves of Figure 1a, the numerical solution in this case made use of the rate constants: $k_M = 4.14 \times 10^6$ s$^{-1}$ and $k_E = 1.93 \times 10^7$ s$^{-1}$. Due to the deactivation of excimers and monomers, the readings of $S(R,t)$, especially ~3.9 Å, are seen to be lower than those in Figure 1a.

If $S(R,t)$ is known, the probability of finding excimers in the system at time $t$ is

$$S_E(t) = \int_0^{R_m} S(R,t)\, dR + \int_{R_m}^{m_x} X(R)\, S(R,t)\, dR \quad (27)$$

The probability of finding monomer M* is then

$$S_M(t) = \int_{R_m}^{m_x} (1 - X(R)) S(R,t)\, dR \quad (28)$$

These probabilities are proportional to intensities $I_E(t)$ and $I_M(t)$ of fluorescence emission from excimers and monomers at time $t$, respectively.

## III. Computational Techniques

**Numerical Solution for $S_M(t)$ and $S_E(t)$.** Computation was performed on an IBM RISC system/6000 Model 320 workstation. For a chain of the contour length, $m_x$, of 200 Å, 10 min is usually required to simulate the results of $10^7$ jumps of the jump distance of 0.2 Å. Obviously, as $\delta_R$ increases, the contour length of the chain is divided into fewer divisions and thus less computational time is needed. The main advantage of using larger $\delta_R$ values, however, derives from the fact that $\psi$, according to eq 19, decreases inversely to the second power of $\delta_R$ for a given $D$ value. Thus, a larger $\delta_R$ corresponds to a smaller $\psi$ and thus fewer jump steps for a given delay time $t$ after the pulse excitation. However, the use of too large a $\delta_R$ results in inaccuracy in $S(R,t)$. The optimal $\delta_R$ value was found to be between 0.15 and 0.20 Å. The $\delta_R$ value of 0.20 Å was used in most of our numerical calculations. The $\delta_R$ value of 0.15 Å was used only if the value of 0.20 Å was found to give insufficiently accurate results.

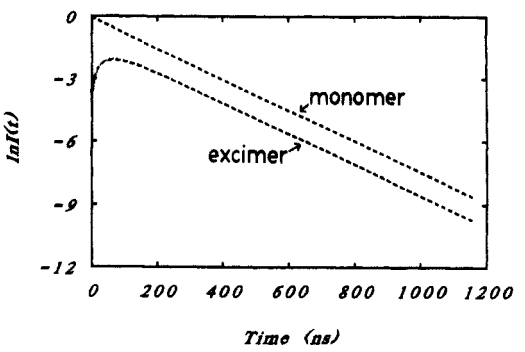


**Figure 2.** Best fits, curves (···), to the $S_M(t)$ and $S_E(t)$ curves, (- - -), generated from eqs 27 and 28 of the Liu and Guillet theory by eqs 1 and 2 of the Birks scheme.

**Fitting of $S_M(t)$ or $S_E(t)$ with Eq 1 or 2.** The fitting of transient intensity profiles, i.e., $S_M(t)$ or $S_E(t)$ generated from the Liu and Guillet theory, using eq 1 or 2 is achieved with a program which minimizes $\chi^2$, the square of the percentage error in fitting:

$$\chi^2 = [\Delta I(t)/I(t)]^2 \quad (29)$$

In eq 29, $I(t)$, $S_E(t)$, or $S_M(t)$, computed from the L–G theory using eq 27 or 28, is the probability of finding excimers or monomers in the system at time $t$; $\Delta I(t)$ is the difference between $I(t)$ computed from the L–G theory and that calculated using eq 2 or 1.

In analogy to data from a TCSPC measurement, a typical $S_M(t)$ or $S_E(t)$ curve consists of 250–500 data points. The sum of $S_M(t)$ and $S_E(t)$ at $t = 0$ is normalized to 1. In the last channel, the $S_M(t)$ value should be ~0.001. The time interval between two adjacent data points is usually $\tau_M/100$. Figure 2 illustrates such a fit. Curves (- - -) are the transient monomer and excimer emission intensity profiles generated from the L–G theory. The curves were generated by assuming that $R_n = 67.6$ Å, $m_x = 350$ Å, $D = 3.0 \times 10^{-6}$ cm$^2$/s, $m = 10$, $n = 3$, $\epsilon_0/k_BT = 8.05$, $R_0 = 3.6$ Å, $\tau_M = 242.8$ ns, and $\tau_E = 58.1$ ns. Curves (···) are the best fit to the above transient profiles using eqs 1 and 2. Excellent fit is obtained for the monomer decay. In cases when the Birks scheme works, the typical $\chi^2$ obtained from fitting monomer decay curves is $10^{-6}$–$10^{-7}$. This explains why one cannot see the monomer decay curve (···) in Figure 2, because the fit is so good and the monomer decay curve (···) is completely buried in the monomer decay curve (- - -). The excimer intensity profile from the L–G theory and that calculated using eq 2 agree with each other very well as well. The typical $\chi^2$ for fitting excimer transient intensity profiles is ~$10^{-4}$–$10^{-5}$.

## IV. An Interpretation of the Birks Scheme

**Validity of the Birks Scheme.** As will be explained later, the various parameters used above for generating the $S_M(t)$ and $S_E(t)$ curves are typical of those for excimer formation and dissociation involving pyrene groups attached to ends of polystyrene chains of the molecular weight 9200 studied by Winnik et al.[1] The curves generated can be fitted using eq 1 or 2. The fitting parameters $\lambda_1$, $\lambda_2$, $\lambda_3$, $\lambda_4$, $A_1$, $A_2$, $A_3$, and $A_4$ thus produced

**Table I**
**Parameters $\lambda_1$, $A_1$, $\lambda_2$, $A_2$, $\lambda_3$, $A_3$, $\lambda_4$, and $A_4$ Generated from Fitting $S_M(t)$ and $S_E(t)$ Curves Shown in Figure 2 Using Equations 1 and 2 of the Birks Scheme[a]**

| monomer | | | | | excimer | | | | |
|---|---|---|---|---|---|---|---|---|---|
| $A_1$ | $\lambda_1 \times 10^{-7}$ ($s^{-1}$) | $A_2$ | $\lambda_2 \times 10^{-7}$ ($s^{-1}$) | $\chi^2 \times 10^7$ | $A_3$ | $\lambda_3 \times 10^{-7}$ ($s^{-1}$) | $A_4$ | $\lambda_4 \times 10^{-7}$ ($s^{-1}$) | $\chi^2 \times 10^5$ |
| 0.921 | 0.727 | 0.061 | 2.32 | 3.4 | 0.288 | 0.726 | −0.275 | 2.22 | 0.91 |

[a] $S_M(t)$ and $S_E(t)$ curves generated using $R_n$ = 67.6 Å, $m_x$ = 350 Å, $D = 3.0 \times 10^{-6}$ $cm^2/s$, $m$ = 10, $n$ = 3, $\epsilon_0/k_BT$ = 8.05, $\tau_M$ = 242.8 ns, and $\tau_E$ = 58.1 ns.

**Table II**
**Effect of the Variation of $\tau_M$ on the Validity of the Birks Scheme[a]**

| $\tau_M$ (ns) | $A_1$ | $\lambda_1 \times 10^{-7}$ ($s^{-1}$) | $A_2$ | $\lambda_2 \times 10^{-7}$ ($s^{-1}$) | $k_1 \times 10^{-7}$ ($s^{-1}$) | $k_{-1} \times 10^{-6}$ ($s^{-1}$) | $k_E \times 10^{-7}$ ($s^{-1}$) | $A_3$ | $\lambda_3 \times 10^{-7}$ ($s^{-1}$) | $A_4$ | $\lambda_4 \times 10^{-7}$ ($s^{-1}$) |
|---|---|---|---|---|---|---|---|---|---|---|---|
| 25 | 0.071 | 2.13 | 0.878 | 5.89 | | | | 0.382 | 1.85 | −0.358 | 7.50 |
| 50 | 0.148 | 1.84 | 0.791 | 3.88 | | | | 0.686 | 1.76 | −0.656 | 4.43 |
| 70 | 0.202 | 1.68 | 0.734 | 3.32 | | | | 0.865 | 1.64 | −0.830 | 3.65 |
| 100 | 0.278 | 1.58 | 0.654 | 2.94 | 1.53 | 2.51 | 1.73 | 1.066 | 1.57 | −1.026 | 3.11 |
| 150 | 0.394 | 1.53 | 0.539 | 2.70 | 1.54 | 2.17 | 1.81 | 1.215 | 1.51 | −1.172 | 2.83 |
| 300 | 0.494 | 1.36 | 0.435 | 2.43 | 1.53 | 1.87 | 1.74 | 1.358 | 1.36 | −1.305 | 2.48 |

[a] $S_M(t)$ and $S_E(t)$ curves generated using $R_n$ = 38.6 Å, $D = 2.0 \times 10^{-6}$ $cm^2/s$, $\tau_E$ = 58.1 ns, $n$ = 3, $m$ = 10, $R_0$ = 3.0 Å, and $\epsilon_0/k_BT$ = 8.45.

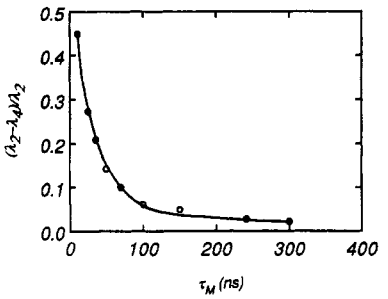


**Figure 3.** Plot of $(\lambda_2 - \lambda_4)/\lambda_2$ as a function of fluorescence lifetimes, $\tau_M$, of monomers. Parameters $\lambda_2$ and $\lambda_4$ are obtained when eqs 1 and 2 are used to fit $S_M(t)$ and $S_E(t)$ curves generated from using eqs 28 and 27 and different $\tau_M$ values.

are listed in Table I. They obey relations 3a–c within ±4% of error. The Birks scheme is thus proved applicable within experimental error in this case as was found by Winnik et al.[1]

The solutions of $S_M(t)$ and $S_E(t)$ are determined by the choice of the excimer interaction potential and the values of $D$, $R_n$, $\tau_M$, and $\tau_E$ used. The excimer interaction potential has been assumed to possess the general form as given by eq 15 in which four parameters, $n$, $m$, $R_0$, and $\epsilon_0$, are contained. In total, there are eight parameters which determine the shape of the $S_M(t)$ and $S_E(t)$ curves. The $S_M(t)$ and $S_E(t)$ curves are generated each time with a given set of parameters. The parameters can then be varied and new $S_M(t)$ and $S_E(t)$ curves are generated. The newly generated curves can be further tested to see whether they can be fitted by the Birks scheme. In this way, the effect of the variation in seven of the eight parameters excluding $R_0$ on the validity of the Birks scheme will be examined in the sections to follow. The effect of varying $R_0$ is not examined because $R_0$, in reality, can only assume values out of a very limited range.

Listed in Table II are the $\lambda_1$, $\lambda_2$, $\lambda_3$, $\lambda_4$, $A_1$, $A_2$, $A_3$, and $A_4$ parameters obtained from fitting $S_M(t)$ and $S_E(t)$ curves generated using eqs 28 and 27 and different $\tau_M$ values. As $\tau_M$ increases, the agreement between $\lambda_1$ and $\lambda_3$ or $\lambda_2$ and $\lambda_4$ improves or the Birks scheme works better. The variation of $(\lambda_2 - \lambda_4)/\lambda_2$ as a function of $\tau_M$ is illustrated in Figure 3. Though the data are not shown, a similar trend was observed when $\tau_E$ increased. The conclusion is that the Birks scheme works better when $\tau_M$ or $\tau_E$ values are large.

The same conclusion was reached by the Wilemski and Fixman (W–F) theory, which predicts that the fluorescence quenching process can be described approximately by a single rate constant at times which are considered sufficiently long after the pulse excitation. A typical transient monomer fluorescence intensity profile from a TCSPC measurement registers the decay of monomer intensity from the initial normalized intensity of 1 to the final intensity of $10^{-3}$. Increasing the lifetime $\tau_M$ of monomer fluorescence or the lifetime $\tau_E$ of excimer fluorescence can extend the time range in which the kinetics of excimer formation and dissociation is studied. When fitting the decay curves of monomer or excimer emission intensity over a longer time interval in which the intensity of monomer intensity is decreased by 1000-fold, the contribution of short-time behavior to the overall kinetics becomes less important. So, as $\tau_M$ or $\tau_E$ increases, one expects that the Birks scheme works better.

The effect of the variation in $D$ and $R_n$ on the validity of the Birks scheme was examined. It was revealed that small $D$ and large $R_n$ can lead to the failure of the Birks scheme. The relative magnitude of the rate of monomer or excimer deactivation to that of internal relaxation of the connecting chain appears to determine whether the Birks scheme is applicable. The longest internal relaxation time $\tau_1$ for a polymer chain described by the harmonic spring model is defined by[7–9]

$$\tau_1 = R_n^2/(3D) \tag{30}$$

For the Birks scheme to be valid, it is preferred to have both lifetimes of monomer and excimer emission much larger, e.g., at least 2–3 times larger, than $\tau_1$. However, when one of the lifetimes is slightly smaller than $\tau_1$, the other one should be much larger than $\tau_1$ so that the overall rate for excimer and monomer deactivation is comparable to the rate of chain relaxation. In conclusion, if $\tau_M$ and $\tau_E$ are fixed, increasing $\tau_1$ in whichever way, e.g., by decreasing $D$ or increasing $R_n$, can eventually make the rate of chain relaxation slower than the overall rate of deactivation and thus leads to the breakdown of the Birks scheme.

The excimer interaction potential has been shown to have a large effect on the shape of the transient excimer and monomer intensity profiles but have little effect on the validity of the Birks scheme as long as $\tau_E$ and $\tau_M$ are much larger than $\tau_1$. The effect of varying $\epsilon_0$, $n$, and $m$ on the magnitude of rate constants $k_1$ and $k_{-1}$ will be discussed in the next two sections.

Table III
Variation of $k_1$ and $k_{-1}$ as a Function of $D$ or $R_n$[a]

| $D$ varies and $R_n$ = 38.6 Å | | | | $R_n$ varies and $D = 2.8 \times 10^{-6}$ cm²/s | | | |
|---|---|---|---|---|---|---|---|
| $D \times 10^6$ (cm²/s) | $D/R_n^3 \times 10^{-13}$ (cm⁻¹·s⁻¹) | $k_1 \times 10^{-7}$ (s⁻¹) | $k_{-1} \times 10^{-6}$ (s⁻¹) | $R_n$ (Å) | $D/R_n^3 \times 10^{-13}$ (cm⁻¹·s⁻¹) | $k_1 \times 10^{-7}$ (s⁻¹) | $k_{-1} \times 10^{-6}$ (s⁻¹) |
| 1.5 | 2.61 | 1.16 | 1.27 | 67.6 | 0.91 | 0.41 | 2.60 |
| 2.0 | 3.48 | 1.54 | 2.01 | 57.4 | 1.48 | 0.64 | 2.09 |
| 3.0 | 5.22 | 2.28 | 3.46 | 47.7 | 2.58 | 1.10 | 2.33 |
| 4.0 | 6.96 | 3.03 | 4.95 | 44.5 | 3.18 | 1.36 | 2.44 |
| 5.0 | 8.70 | 3.79 | 6.53 | 38.6 | 4.87 | 2.11 | 3.17 |
| 10.0 | 17.4 | 7.53 | 14.2 | | | | |

[a] $S_M(t)$ and $S_E(t)$ curves generated using $\tau_M$ = 241.8 ns, $\tau_E$ = 58.1 ns, $n$ = 3, $m$ = 10, and $\epsilon_0/k_BT$ = 8.45.

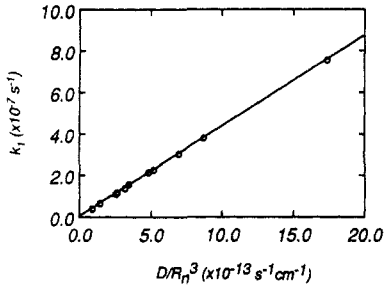


**Figure 4.** Plot of $k_1$, obtained from fitting $S_M(t)$ and $S_E(t)$ curves generated from eqs 28 and 27 of the Liu and Guillet theory with eqs 1 and 2 of the Birks scheme, as a function of $D/R_n^3$. The coefficient, $D$, of relative diffusion between polymer chain ends and the root-mean-square end-to-end distances, $R_n$, are parameters inputted to generate $S_M(t)$ and $S_E(t)$ curves.

**Rate Constant $k_1$.** In Table II, the effect of varying $\tau_M$ on the magnitude of $k_1$ is illustrated. The Birks scheme seems valid if $\tau_m$ is larger than 100 ns. In cases when the Birks scheme holds, eqs 4 and 5 were used to calculate rate constants $k_1$, $k_{-1}$, and $k_E$ from fitting parameters $\lambda_1$, $\lambda_2$, and $A_1/A_2$. The $k_E$ values were found not to vary with $\tau_M$ within the error associated with the use of eqs 1 and 2 to approximate the $S_M(t)$ and $S_E(t)$ curves and compare well with the inputted $k_E$ value, $1.72 \times 10^7$ s$^{-1}$. The value of $k_1$ does not vary with $\tau_M$ either. As the rate constant $k_1$ is obtained from fitting $S_M(t)$ and $S_E(t)$ curves generated from equations of the L–G theory using the Birks scheme, the invariability in $k_1$ with $\tau_M$ is thus the prediction of the L–G theory. The same conclusion is reached by the W–F theory. The rate constant for fluorescence quenching, derived from the W–F theory using the harmonic spring model, is given by eq 9 in the limit of $R_e/R_n \to 0$. Since $R_e$, $R_n$, and $D$ are fixed in eq 9, $k_1$ should not vary with $\tau_M$.

In Table III, the effect of varying $D$ and $R_n$ on the magnitude of $k_1$ is illustrated. The values of $k_1$ increase with $D$. The increase of $k_1$ with $D$ is expected due to the fact that excimer formation is diffusion-controlled, and an increase in the diffusion coefficient naturally leads to an increase in the rate constant.

The $k_1$ values decrease with $R_n$. The W–F theory predicts that when $k_1$ is plotted versus $D/R_n^3$, a straight line should be obtained. This was done for $k_1$ values of Table III obtained from varying $D$ and $R_n$, and a straight line was indeed obtained as shown in Figure 4. The best fit to the data points is

$$k_1 = 8.764 \times 10^4 + 4.329 \times 10^{-7} D/R_n^3 \qquad (31)$$

where $D$ is in cm²/s, $R_n$ in cm, and $k_1$ in s⁻¹. From the slope, $R_e$ of eq 9 was calculated to be 12.8 Å.

The observation is important. The $k_1$ values of Table III were obtained from fitting $S_M(t)$ and $S_E(t)$ curves generated from the L–G theory using the Birks scheme. They obey the relation given by eq 9 derived from the W–F theory. This indicates that the final expression for $k_1$ should be very similar in form for both The L–G theory and the W–F theory despite the apparent differences between the two approaches: The L–G theory uses an excimer interaction potential to govern excimer formation. The W–F theory assumes that excimers are formed as soon as the end groups are within an effective reaction radius $R_e$.

The shape of the excimer interaction potential has been demonstrated not to affect the validity of the Birks scheme. Here, two potentials of different shapes are shown to be quantitatively equivalent in describing excimer formation if the adjustable parameter $R_e$ of eq 9 is chosen properly. What these results suggests to us is that when solving eqs 27 and 28 analytically for $S_E(t)$ and $S_M(t)$, the $n$ and $m$ parameters of eq 15 can be assigned values for the convenience of mathematical derivations. The final expression for $k_1$ may not be affected as long as $\epsilon_0$ is left as an adjustable parameter, because errors in the assignment of $n$ and $m$ values can be compensated by an error in $\epsilon_0$.

The increase in $\epsilon_0$, i.e., increasing the depth of the potential well, leads to larger $k_1$ values (Table IV). The increase in the value of $k_1$ with $\epsilon_0$ seems to contradict the definition of a diffusion-controlled reaction, because the rate of such a reaction is deemed to be determined by $D$ and not to be determined by $\epsilon_0$. In conventional theories,[18] the energy factor is not involved. What is used is $R_e$, the effective reaction radius within which a chemical reaction between two molecules occurs instantaneously. The magnitude of $R_e$ is determined by $\epsilon_0$. As $\epsilon_0$ increases, $R_e$ increases and so does $k_1$. The $R_e$ values shown in Table IV are calculated using eq 9 and the $k_1$ values tabulated in column 2 of the table.

Table IV also shows the variation of $k_1$ with $n$ and $m$. Decreasing the $n$ value extends the attractive range of the excimer formation free energy. Thus, as expected, smaller $n$ values lead to larger $k_1$ values. The variation of $m$ from 8.5 to 11 barely affected the magnitude of $k_1$ values. This is understandable, as $k_1$ characterizes the rate at which the end groups come together. The rate should be mainly determined by the attractive part of the interaction potential.

**Rate Constant $k_{-1}$ and Ratio $k_1/k_{-1}$.** The value of $k_{-1}$ in Table II was found to increase on increasing $k_M$. Further examination showed that $k_{-1}$ decreased if $k_E$ increases (Table V).

The variation of $k_{-1}$ with $k_M$ or $k_E$ is not expected. Conventionally, $k_{-1}$ has been assumed to be an intrinsic first-order rate constant, which implies that $k_{-1}$ should be independent of factors such as the chain length and the magnitudes of $\tau_M$ and $\tau_E$. An intrinsic rate constant should depend on the intrinsic properties of an excimer.

Winnik et al.[1] studied a limited number of samples of different molecular weights and observed that $k_{-1}$ varied within ±30% (Table VII). They thus concluded that $k_{-1}$ was the intrinsic rate constant for excimer dissociation. They further suggested that the ratio $k_1/k_{-1}$ should be

Table IV
Variation of $k_1$ and $k_{-1}$ as a Function of $\epsilon_0$, $n$, and $m$

| $\epsilon_0$ varies[a] | | | | $n$ varies[b] | | | $m$ varies[c] | | |
|---|---|---|---|---|---|---|---|---|---|
| $\epsilon_0/k_BT$ | $k_1 \times 10^{-7}$ ($s^{-1}$) | $k_{-1} \times 10^{-6}$ ($s^{-1}$) | $R_e$ (Å) | $n$ | $k_1 \times 10^{-7}$ ($s^{-1}$) | $k_{-1} \times 10^{-6}$ ($s^{-1}$) | $m$ | $k_1 \times 10^{-7}$ ($s^{-1}$) | $k_{-1} \times 10^{-6}$ ($s^{-1}$) |
| 6 | 1.17 | 16.5 | 9.9 | 2.0 | 2.46 | 1.71 | 11 | 1.54 | 1.59 |
| 7 | 1.35 | 7.01 | 11.5 | 2.5 | 1.88 | 1.62 | 10.5 | 1.54 | 1.76 |
| 8.45 | 1.53 | 1.90 | 13.0 | 3.0 | 1.53 | 1.90 | 10 | 1.53 | 1.90 |
| 9 | 1.59 | 1.25 | 13.5 | 3.5 | 1.32 | 2.33 | 9.5 | 1.53 | 2.20 |
| 10 | 1.68 | 0.62 | 14.3 | 4.0 | 1.16 | 3.24 | 9 | 1.52 | 2.34 |
| 25 | 2.43 | 0.17 | 20.6 | 4.5 | 1.05 | 4.15 | 8.5 | 1.51 | 2.73 |

[a] The $S_M(t)$ and $S_E(t)$ curves are generated using $R_n$ = 38.6 Å, $D = 2.0 \times 10^{-6}$ $cm^2/s$, $\tau_M$ = 241.8 ns, $\tau_E$ = 58.1 ns, $R_0$ = 3.6 Å, $n$ = 3, and $m$ = 10. [b] The same parameters as in case $a$ are used except that $\epsilon_0/k_BT$ = 8.45 and $n$ varies. [c] The same parameters as in csae $b$ are used except that $n$ = 3 and $m$ varies.

Table V
Variation of $k_{-1}$ with $\tau_M$ and $\tau_E$

| | $k_{-1} \times 10^{-6}$ ($s^{-1}$) | | | | |
|---|---|---|---|---|---|
| $\tau_E$ (ns) | $\tau_M$ = 150 ns | $\tau_M$ = 24.18 ns | $\tau_M$ = 350 ns | $\tau_M$ = 450 ns | $\tau_M$ = 550 ns |
| 60 | 2.19 | 1.96 | 1.86 | 1.78 | 1.76 |
| 100 | 2.80 | 2.56 | 2.43 | 2.36 | 2.33 |
| 200 | 3.28 | 3.03 | 2.90 | 2.84 | 2.80 |
| 300 | 3.44 | 3.18 | 3.06 | 3.00 | 2.96 |
| 400 | 3.52 | 3.27 | 3.14 | 3.08 | 3.04 |
| 500 | 3.58 | 3.32 | 3.19 | 3.13 | 3.09 |

[a] The $S_M(t)$ and $S_E(t)$ curves are generated using $R_n$ = 38.6 Å, $D = 2.0 \times 10^{-6}$ $cm^2/s$, $R_0$ = 3.6 Å, $n$ = 3, $m$ = 10, and $\epsilon_0/k_BT$ = 8.45.

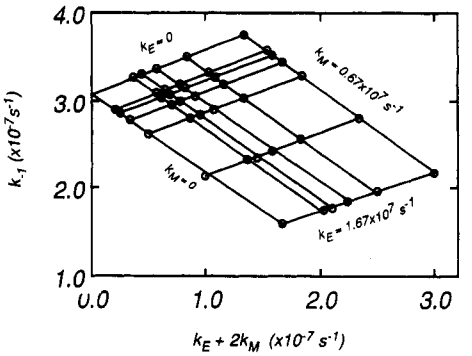


Figure 5. Plot of $k_{-1}$ as a function of $k_E + 2k_M$.

equal to the equilibrium constant for excimer formation and dissociation. Since both $k_1$ and $k_{-1}$ were assumed to be independent of $\tau_M$ and $\tau_E$, the ratio $k_1/k_{-1}$ has thus been assumed implicitly to be independent of $\tau_M$ and $\tau_E$.

The L–G theory clearly suggests that $k_{-1}$ depends on $k_M$ and $k_E$ as shown in Table V. The excimer dissociation here is assumed to occur if the two ends diffuse away from one another. The diffusion of the chain ends is to ensure that the equilibrium relative concentration of excimers to monomers is achieved and maintained. The actual relative monomer to excimer concentration is determined by three concurrent processes: i.e., the end-group diffusion, monomer deactivation, and excimer deactivation. Depending on the magnitudes of $k_E$, $k_M$, and $D$, the required equilibrium between excimers and monomers may never be achieved. If excimers, for example, deactivate much faster than their formation, the ratio of excimer to monomer concentration is constantly lower than the equilibrium concentration ratio. In this case the excimers are less likely to dissociate, and the rate constant for excimer dissociation is lower than the equilibrium value. The rate constant $k_{-1}$ should increase with $\tau_E$ if $\tau_M$ is constant. This is exactly what is observed in Table V. If $\tau_E$ is fixed, decreasing $k_M$ shifts the equilibrium between excimers and monomers to favor excimer formation but to disfavor excimer dissociation. The rate of excimer formation is diffusion-controlled and thus $k_1$ cannot be further increased by changing the value of $\tau_M$. Increasing $\tau_M$ therefore only results in the decrease in $k_{-1}$ values.

Since $k_{-1}$ varies with $\tau_M$ and $\tau_E$, the ratio $k_1/k_{-1}$ varies as well. The ratio determined from a kinetic experiment thus does not necessarily represent the equilibrium constant between excimer formation and dissociation. The ratio approaches the equilibrium constant only when $1/\tau_M$ and $1/\tau_E$ both approach zero or at least the internal relaxation rate of the chain is much faster than the deactivation processes so that the equilibrium between excimers and monomers is constantly maintained.

The $k_{-1}$ value in the limit of $\tau_M \to \infty$ and $\tau_E \to \infty$ can be obtained by plotting $k_{-1}$ of Table V versus $k_E + 2k_M$ as shown in Figure 5. The group of lines with negative slopes depict the dependence of $k_{-1}$ on $k_E$. The group of lines with positive slopes illustrate the dependence of $k_{-1}$ on $k_M$. The $k_{-1}$ value in the limit of $\tau_M \to \infty$ and $\tau_E \to \infty$ can be extrapolated in two ways. One way is to start with the extrapolation of $k_{-1}$ values in the limit of $\tau_M \to \infty$ for various $1/\tau_E$ values. Plotting the extrapolated $k_{-1}$ values versus $1/\tau_E$ and extrapolating to the limit $1/\tau_E \to 0$ yields the desired $k_{-1}$ value for the limit $\tau_M \to \infty$ and $\tau_E \to \infty$. Or by taking the other approach, one starts with the extrapolation of $k_{-1}$ values in the limit of $\tau_E \to \infty$ for various $1/\tau_M$ values and then plots the extrapolated $k_{-1}$ values versus $1/\tau_M$ to obtain $k_{-1}$ in the limit $\tau_M \to \infty$ and $\tau_E \to \infty$. The same $k_{-1}$ value, $3.075 \times 10^6$ $s^{-1}$, for the limit $\tau_M \to \infty$ and $\tau_E \to \infty$ was obtained from the two different approaches. Since $k_1$ was found to be independent of $\tau_M$ and $\tau_E$ and equal to $1.54 \times 10^7$ $s^{-1}$, the equilibrium constant for excimer formation and dissociation for the chain defined above is thus 5.01.

Provided that neither monomer nor excimer deactivates to the ground state, the equilibrium constant is related to the probability, $S_E(t\to\infty)$, of finding excited end chromophores as excimers long after pulse excitation by

$$k_1/k_{-1} = S_E(t\to\infty)/S_M(t\to\infty) \qquad (32)$$

where $S_M(t\to\infty)$, equal to $1 - S_E(t\to\infty)$, is the probability of finding excited end chromophores existing as monomers at equilibrium. Using the above equation and $k_1/k_{-1}$ = 5.01, $S_E(t\to\infty)$ was found to be 83.4%.

The value of $S_E(t\to\infty)$ can also be calculated from another approach. The equilibrium end-to-end distance distribution function with interacting end groups is given by eq 13. Interesting eq 13 into eq 27 to replace $S(R,t)$ yields the equilibrium probability, $S_E(t\to\infty)$, of finding excimers in the system. The value of $S_E(t\to\infty)$ calculated from this approach using parameters originally inputted to generate the $S_M(t)$ and $S_E(t)$ curves is 84.2%. The value 84.2% is very close to 83.4%. The slight difference might be due to the use of the Birks scheme in describing the kinetics of excimer formation and dissociation.

Then $k_{-1}$ of Table III was found to increase on increasing $D$. The excimer dissociation reaction is controlled both by the excimer interaction potential and by the diffusivity of the chain end. That a higher diffusivity leads to a higher rate constant is not surprising.

The value of $k_1/k_{-1}$ was observed, in Table III, to decrease with increasing $D$. In the discussed case, $\tau_E$ is shorter than $\tau_M$, and the rate of excimer formation is not much faster than the rate of excimer deactivation. The concentration ratio of excimer to monomer at any given time $t$ is expected to be lower than its equilibrium value. The trend for excimers to back-dissociate into monomers is reduced and so is $k_{-1}$ relative to its equilibrium value. Therefore, the ratio $k_1/k_{-1}$ is larger when $D$ is small. The ratio is expected to approach the equilibrium value as $D$ approaches infinity.

The value of $k_{-1}$ in Table III was found to vary with $R_n$. This again contradicts the concept of an intrinsic rate constant $k_{-1}$ in conventional theory. As $R_n$ increased from 38.6 to 67.6 Å, $k_{-1}$ varied within ±26%, which is coincidentally close to the error, ±30%, observed by Winnik et al. for their samples.

As $\epsilon_0$ increases, $k_{-1}$ decreases as shown in Table IV. Since $k_1$ increases with $\epsilon_0$, the ratio $k_1/k_{-1}$ increases with $\epsilon_0$, as expected.

The decrease in $n$ extends the range of the attractive part of the excimer interaction potential and thus decreases $k_{-1}$ values as shown in Table IV. Larger $m$ values lead to smaller $k_{-1}$ values due to the fact that larger $m$ values make the repulsive part of the excimer interaction potential even more short-ranged. The fitting parameters $A_1$, $\lambda_1$, $A_2$, and $\lambda_2$ did not change significantly as $m$ varied from 8.5 to 11. This is important because it means that the shape of the transient intensity curves is not affected by the value of $m$ to a large degree. Thus an uncertainty in the assignment of $m$ value will not introduce significant error to the final shape of the transient intensity curves.

## V. Fitting of Previous Data Using the Liu–Guillet Model

The previous section compared the L–G theory to the Birks scheme in general. In this section, the data of Winnik et al.[1] will be treated using the L–G theory to generate the coefficient of relative diffusion, $D$, between polymer chain ends. As mentioned before, the partial differential diffusion–reaction equation derived from eq 25 of the L–G theory has not been solved analytically, and no explicit functional forms are available for $S_M(t)$ and $S_E(t)$. The transient intensity profiles of excimer and monomer emission experimentally monitored cannot be fitted directly using eqs 27 and 28. Fortunately, the Birks scheme has been shown to be valid in this case by Winnik et al.[1] They have determined the fitting parameters $\lambda_1$, $\lambda_2$, $\lambda_3$, $\lambda_4$, $A_1/A_2$, and $A_3/A_4$. What is needed is to generate the $S_M(t)$ and $S_E(t)$ curves using eqs 28 and 27 and to fit the curves generated using eq 1 or 2 depending on whether the transient monomer or excimer profile is fitted. If the parameters $\lambda_1$, $\lambda_2$, $\lambda_3$, $\lambda_4$, $A_1/A_2$, and $A_3/A_4$ obtained from fitting the transient profiles generated from eqs 27 and 28 agree with those obtained by Winnik et al., the fitting of experimental decay curves using the L–G theory is achieved.

As mentioned, there are eight parameters which determine the shape of $S_M(t)$ and $S_E(t)$ curves. Fortunately, many of the eight parameters can be determined independently. The following few sections discuss the assignment of seven of the eight parameters. $D$ will be left as an adjustable parameter so that different $S_M(t)$ and $S_E(t)$ curves can be generated for fitting by eqs 1 and 2.

**Table VI**
**Decay Constants for Decay of Monomer and Excimer Fluorescence Measured by Winnik et al. for Pyrene-Terminated Polystyrene**

| $\bar{M}_n$ | $R_n$ (Å) | $\lambda_1 \times 10^{-7}$ ($s^{-1}$) | $\lambda_2 \times 10^{-7}$ ($s^{-1}$) | $A_1/A_2$ | $\lambda_3 \times 10^{-7}$ ($s^{-1}$) | $\lambda_4 \times 10^{-7}$ ($s^{-1}$) | $A_3/A_4$ |
|---|---|---|---|---|---|---|---|
| 2900 | 38.6 | 1.20 | 2.54 | 1.594 | 1.43 | 2.70 | −0.98 |
| 3900 | 44.5 | 1.13 | 2.52 | 0.521 | 1.21 | 2.44 | −0.97 |
| 4500 | 47.7 | 1.01 | 2.26 | 0.362 | 1.12 | 2.33 | −0.97 |
| 6600 | 57.4 | 0.83 | 2.48 | 0.112 | 0.87 | 2.14 | −0.96 |
| 9200 | 67.6 | 0.66 | 2.04 | 0.099 | 0.72 | 2.14 | −0.95 |

**Previous Data.** The molecular weights of the samples studied by Winnik et al. are shown in Table VI. All samples possessed low polydispersity, i.e., <1.10. Data obtained by carrying out the study in cyclohexane at 34.5 °C, a Θ solvent for polystyrene, will be treated.

The transient intensity profiles of monomers and excimers of all samples listed in Table VI could be fitted using eqs 1 and 2. Values of $\lambda_1$, $\lambda_2$, $\lambda_3$, $\lambda_4$, $A_1/A_2$, and $A_3/A_4$ measured by Winnik et al. are reproduced in Table VI. Using eqs 4 and 5, the values of $k_1$, $k_{-1}$, and $\tau_E$ were calculated. The $k_1$ and $k_{-1}$ values are listed in Table VII. The $\tau_E$ value was found to be 58.1 ns and independent of molecular weight.

**Calculation of $R_n$.** Standard techniques such as light scattering and viscometry can be used to determine the $R_n$ values of polymer chains.[14] In fact, for polystyrene dissolved in cyclohexane at 34.5 °C, $R_n$ for samples of moderately high molecular weight, e.g., >8000, can be calculated using[19]

$$R_n = 5.04N^{1/2}\ (\text{Å}) \tag{33}$$

where $N$ is the number of bonds in the polymer chain. Using eq 33, the $R_n$ value for each sample was calculated and listed in Table VI. Since the molecular weights of the samples used by Winnik and co-workers are low, relatively large errors may be associated with the $R_n$ values calculated.

**Determination of $\tau_M$ and $\tau_E$.** The $\tau_M$ value can be measured by using a reference sample which bears only one end chromophore. This value was determined by Winnik et al. to be 241.8 ns for a pyrene group attached to the end of polystyrene solubilized in cyclohexane at 34.5 °C.

The lifetime, $\tau_E$, of the excimer can, in principle, be determined from a sample which contains pyrene molecules all locked in the excimer conformation when dissolved in cyclohexane. This is difficult to achieve experimentally. In this case, the Birks scheme works well and $\tau_E$ can be obtained by treating the kinetic data using the Birks scheme. The value was found to be 58.1 ns by Winnik and co-workers.[1]

The L–G scheme seems to depend on the validity of the Birks scheme. This is due to restriction that analytic solutions for $S_M(t)$ and $S_E(t)$ have not been possible at this stage. If $S_M(t)$ and $S_E(t)$ can be solved and be expressed, for example, as a sum of exponential terms, $\sum_i a_i \exp(-k_i t)$, up to four $k_i$ values can be determined from curve fitting. If the relationship between $k_i$ and the aforementioned eight parameters is derived, the four $k_i$ values can at least be used to determine four of the eight parameters. Thus, $\tau_E$ can, in principle, be determined from the L–G scheme independently.

**Pyrene Excimer Formation Potential.** The attractive part of the interaction energy potential between two parallel pyrene rings was experimentally shown by Birks to be inversely proportional to the third power of the

Table VII
Comparison of Parameters $\lambda_1$, $\lambda_2$, $\lambda_3$, $\lambda_4$, and $A_1/A_2$ and Rate Constants $k_1$ and $k_{-1}$ Obtained by Winnik et al. (Exptl) with Those Resulting from Fitting $S_M(t)$ and $S_E(t)$ Curves Generated from the Liu and Guillet Model

| | $\lambda_1$ or $\lambda_3$ ($\times 10^{-7}$ s$^{-1}$) | | $\lambda_2$ or $\lambda_4$ ($\times 10^{-7}$ s$^{-1}$) | | $A_1/A_2$ | | | $k_1$ ($\times 10^{-7}$ s$^{-1}$) | | $k_{-1}$ ($\times 10^{-6}$ s$^{-1}$) | |
|---|---|---|---|---|---|---|---|---|---|---|---|
| $\bar{M}_n$ | exptl | calcd | exptl | calcd | exptl | calcd | $D \times 10^6$ (cm$^2$/s) | exptl | calcd | exptl | calcd |
| 2900 | 1.43 | 1.42 | 2.70 | 2.80 | 1.594 | 1.446 | 2.4 | 1.79 | 1.82 | 2.12 | 2.52 |
| 3900 | 1.21 | 1.27 | 2.44 | 2.32 | 0.521 | 0.552 | 2.5 | 1.21 | 1.23 | 2.79 | 2.04 |
| 4500 | 1.12 | 1.19 | 2.26 | 2.25 | 0.362 | 0.386 | 2.7 | 1.02 | 1.08 | 2.81 | 2.08 |
| 6600 | 0.87 | 0.93 | 2.15 | 2.14 | 0.112 | 0.114 | 2.8 | 0.57 | 0.65 | 2.55 | 2.10 |
| 9200 | 0.72 | 0.80 | 2.14 | 2.16 | 0.099 | 0.077 | 3.5 | 0.42 | 0.49 | 3.95 | 2.71 |

separation distance between them.[2,20] However, the dependence of the free energy of excimer formation on separation distances is of concern here. The free energy of formation and the excimer interaction energy may have different distance dependences. As an approximation, the distance dependence is assumed to be the same for both cases, and $n$ in eq 15 is thus equal to 3.

For two spherical atoms, the repulsive van der Waals interaction energy is usually assumed to be inversely proportional to the twelfth power of their separation distance.[21] For two infinitely large planes, the van der Waals repulsive potential is inversely proportional to the eighth power of $R$.[22,23] Since pyrene contains 16 coplanar carbon atoms and 16 hydrogen atoms, not large enough to be approximated by two infinitely large planes nor small enough to be accepted as two spheric atoms, the $m$ value must lie between 8 and 12. The repulsive interaction free energy is assumed to be inversely proportional to the tenth power of the separation distance between the two planes. This approximation is justified by noting that the variation in $m$ from 8.5 to 11 had little effect on the transient intensity profiles $S_M(t)$ and $S_E(t)$ as discussed previously.

In conclusion, the excimer free energy potential is assumed to be

$$U(R) = -\epsilon_0[2(R_0/R)^3 - (R_0/R)^{10}] \quad (34)$$

The energy minimum has been demonstrated by Birks to be located at ~3.6 Å. This should have been assigned the value of $R_m$. Considering the small difference between $R_0$ and $R_m$ and the relatively large $\delta_R$ values (0.15–0.20 Å) used in computation, the differentiation between $R_0$ and $R_m$ is not of necessity. Furthermore, the kinetic behavior of the system is very unlikely to depend on the location of the energy minimum as long as $R_m$ is much smaller than $R_n$. Thus, the value of 3.6 Å has been used as $R_0$ out of convenience.

The magnitude of $\epsilon_0$ of eq 34 should be roughly equal to the Gibbs free energy of excimer formation from pyrene molecules. The enthalpy $\Delta H$ for excimer formation from pyrene in cyclohexane was determined by Birks[2] as −9.4 kcal/mol. The entropy change $\Delta S$ accompanying the process is −17.6 cal·mol$^{-1}$·K$^{-1}$. The Gibbs free energy for excimer formation at 34.5 °C is calculated using

$$\Delta G = \Delta H - T\Delta S \quad (35)$$

and is −4.0 kcal/mol.

The exact $\epsilon_0$ value can be calculated by realizing that $k_1/k_{-1}$ in the limit of $k_E \to 0$ and $k_M \to 0$ represents the equilibrium constant for excimer formation and dissociation. Using the equilibrium constant measurable experimentally and eq 32, the relative equilibrium excimer concentration, $S_E(t\to\infty)$, can be calculated. As discussed in section IV, $S_E(t\to\infty)$ can also be calculated from using eqs 13 and 27. The values of $S_E(t\to\infty)$ obtained from the latter approach depend on the magnitude of $\epsilon_0$ and should agree with those calculated from the former method. If an $\epsilon_0$ value when inputted leads to an $S_E(t\to\infty)$ value which is the same as that from the former approach, the $\epsilon_0$ value is considered to be the value being sought.

Table VIII
Comparison of $S_E(t\to\infty)$ Values Calculated from Using Equation 46 and Those from Using Equation 32

| $\bar{M}_n$ | $k_1/k_{-1}$[a] | $S_E(t\to\infty)$[a] | $S_E(t\to\infty)$[b] |
|---|---|---|---|
| 2900 | 8.44 | 89.4 | 84.2 |
| 3900 | 4.34 | 81.3 | 80.3 |
| 4500 | 3.63 | 78.4 | 78.2 |
| 6600 | 2.24 | 69.1 | 69.8 |
| 9200 | 1.06 | 51.5 | 60.4 |

[a] Obtained from data of Winnik et al. [b] Obtained from using eqs 23 and 32.

The $k_1/k_{-1}$ values were determined by Winnik et al. for samples of different molecular weights. Those values are, however, not the equilibrium constant due to the fact $\tau_M$ of pyrene monomers and $\tau_E$ of pyrene excimers are not infinitely large. However, it can be shown that $\tau_M$ and $\tau_E$ here are significantly larger than the longest internal relaxation time $\tau_1$ so that $k_1/k_{-1}$ obtained experimentally actually approach the equilibrium constants.

The translational diffusion coefficient, $D_0$, of polystyrene between the molecular weight range of $1.14 \times 10^4$ to $1.04 \times 10^6$ in cyclohexane at 35 °C can be calculated using[19]

$$D_0 = 1.21 \times 10^{-4}\bar{M}_w^{-0.49} \quad (36)$$

According to eq 33, the $R_n$ value of 50 Å corresponds to a molecular weight of ~5000, typical of the molecular weights of the samples studied by Winnik et al. The $D_0$ for samples of this molecular weight range should be ~$2 \times 10^{-6}$ cm$^2$/s. The Kirkwood–Riseman–Flory theory[24,25] requires that the coefficient of end-group diffusion should be larger than the translational diffusion coefficient of the chain as a whole. The theoretical prediction has been demonstrated by the experimental results of L–G.[26] Using the $R_n$ value of 50 Å and the lower limit $D$ value of $2 \times 10^{-6}$ cm$^2$/s, we obtain from eq 30 that $\tau_1 = 41.6$ ns, which is smaller than both $\tau_E$ and $\tau_M$. As an approximation, we assume that $k_1/k_{-1}$ determined by Winnik et al. approaches the equilibrium constants. Using these $k_1/k_{-1}$ values and eq 33, $S_E(t\to\infty)$ values for samples of different molecular weights are calculated and listed in Table VIII. The values are compared with the $S_E(t\to\infty)$ values calculated using eq 13 and 27 and the $\epsilon_0$ value of $8.45k_BT$. The agreement is good for samples of the molecular weights of 3900, 4500, and 6600 and poorer for samples of the molecular weights of 2900 and 9200. For the sample of the molecular weight of 2900, the error is expected to be large due to the fact that the chain is too short to be treated statistically. Then the pyrene end groups are too big for the short chains, and these groups are expected to perturb the Gaussian end-to-end distance distribution function considerably even when they are in the ground state. For the sample of the molecular weight of 9900, the degree of excimer formation is low and a large error is expected from treating experimental data as was commented by Winnik et al. Overall, the agreement between the two sets of $S_E(t\to\infty)$

is considered good. Since the study was carried out at 34.5 °C, the $\epsilon_0$ value corresponds to 5.16 kcal/mol, which is very close to 4.0 kcal/mol calculated from eq 35, considering that the use of $\Delta G$ to approximate $\epsilon_0$ is a very crude approximation because the measurement of $\Delta G$ has implicitly made use of a square well potential for describing excimer formation.

The excimer formation potential is applicable if two planar pyrene groups approach one another face-to-face with overlapping center axes. This is generally not the case when the pyrene groups are far away and their orientations are not correlated. However, as they come closer, the face-to-face relative orientation will be predominant and the assumed functional form for the excimer interaction potential is thus acceptable. The dominance of the face-to-face orientation when two chromophores are close arises from its thermodynamic favorableness and its kinetic feasibility. Thermodynamically, the face-to-face orientation is energetically more stable.[23] Kinetically, the relative rotational motion between chromophores is, in general, faster than the relative diffusional motion.[27] Under this circumstance, the face-to-face orientation can be achieved before two chromophores diffuse too close to one another. This hypothesis is obviously correct by realizing that excimer formation from pyrene is controlled by the rate of translational diffusion and not by the rotational diffusion, which is responsible for the face-to-face relative orientation of an excimer.

**Fitting of Experimental Decay Curves.** Seven of the eight parameters required to describe the kinetics of excimer formation and dissociation involving pyrene groups attached to the opposite ends of polystyrene chains have been assigned values so far. These include $\tau_M$ = 241.8 ns, $\tau_E$ = 58.1 ns, $\epsilon_0 = 8.45 k_B T$, $R_0$ = 3.6 Å, $n$ = 3, and $m$ = 10. The root-mean-square end-to-end distance $R_n$ varies with molecular weight. $R_n$ for each sample is listed in Table VI.

To generate $S_M(t)$ and $S_E(t)$ curves for the sample of the molecular weight of 4500, for example, the $R_n$ value of 47.7 Å was used. With the input of each $D$ value, a set of $S_E(t)$ and $S_M(t)$ curves was generated. Fitting the $S_M(t)$ and $S_E(t)$ curves using eqs 1 and 2 yields fitting parameters $A_1$, $\lambda_1$, $A_2$, $\lambda_2$, $A_3$, $\lambda_3$, $A_4$, and $\lambda_4$. The parameters are compared with those obtained by Winnik et al.[1] When the $D$ value of $2.7 \times 10^{-6}$ cm$^2$/s was used, the best agreement was achieved between the two sets of $A_1$, $\lambda_1$, $A_2$, $\lambda_2$, $A_3$, $\lambda_3$, $A_4$, and $\lambda_4$ parameters. The value of $2.7 \times 10^{-6}$ cm$^2$/s is thus the expected $D$ value.

In Table VII, parameters, $\lambda_1$, $\lambda_2$, $\lambda_3$, $\lambda_4$, and $A_1/A_2$, obtained from fitting $S_M(t)$ and $S_E(t)$ curves generated from the L–G theory and those obtained by Winnik et al. are compared for samples of different molecular weights. The ratio $A_3/A_4$ obtained from the two different approaches are not compared because they both lead to values close to −1 as is required by the Birks scheme. The validity of the Birks scheme requires that $\lambda_1 = \lambda_3$, i.e., the validity of eq 3b. This relation is satisfied by the $\lambda_1$ and $\lambda_3$ parameters that result from fitting $S_M(t)$ and $S_E(t)$ curves generated from the L–G theory within ±0.1%. Those obtained by Winnik et al.[1] do not satisfy eq 3b rigorously, and only the one, either $\lambda_1$ or $\lambda_3$, which is closer to those that result from the former approach is listed in Table VII for comparison. The validity of the Birks scheme also requires that $\lambda_2 = \lambda_4$ or the validity of eq 3c. This relation is only satisified by parameters generated from the two approaches approximately. The $\lambda_2$ and $\lambda_4$ values that result from fitting $S_M(t)$ and $S_E(t)$ curves generated from the L–G theory satisfy eq 3c within the error of ±3%.

**Table IX**
**Comparison between $D$ Obtained from the Wilemski–Fixman Theory and Those from the Liu and Guillet Theory**

| $\bar{M}_n$ | $k_1 \times 10^{-7}$ (s$^{-1}$) | $R_n$ (Å) | $D_{WF} \times 10^6$ (cm$^2$/s) | $D_{LG} \times 10^6$ (cm$^2$/s) |
|---|---|---|---|---|
| 2900 | 1.79 | 38.6 | 2.38 | 2.4 |
| 3900 | 1.21 | 44.5 | 2.46 | 2.5 |
| 4500 | 1.02 | 47.7 | 2.56 | 2.7 |
| 6600 | 0.57 | 57.4 | 2.49 | 2.8 |
| 9200 | 0.42 | 67.6 | 2.99 | 3.5 |

Larger error was seen between the parameters obtained by Winnik et al. Under this circumstance, one $\lambda$ value is picked from each set of $\lambda_2$ and $\lambda_4$ values for comparison. The $\lambda$ values were so chosen that they represent the best agreement between two $\lambda$ values from the two groups.

**Results and Discussion.** The coefficient of relative diffusion between the ends of a polymer chain was obtained as described above. The values of $D$ for chains of different molecular weights are listed in Table VII.

Since $k_1$ is related to $D$ by eq 9, $D$ can also be estimated from $k_1$ values using eq 9. The difficulty associated with the use of this equation lies in the estimation of the value $R_e$. For the current system, we have previously generated $S_M(t)$ and $S_E(t)$ curves using eqs 28 and 27 and different $D$ and $R_n$ values. The curves were then fitted with eqs 1 and 2 to obtain $k_1$ values. From plotting $k_1$ versus $D/R_n^3$, we were able to obtain $R_e$ = 12.8 Å from the slope of the straight line. However, the accuracy of the $R_e$ value generated this way can be questionable because of the different definitions of excimers in the L–G theory and the W–F theory.

Martinho and Winnik have estimated an $R_e$ value of 7.6 ± 0.7 Å from another approach.[28] The difference between 12.8 and 7.6 Å represents a close to 40% error. Since the accuracy of the value of $R_e$ = 7.6 Å is not guaranteed either, $R_e$ = 12.8 Å is then used for calculating $D$ values from $k_1$, and the $D$ values thus calculated are listed in Table IX. The $D$ values are in good agreement with the $D$ values generated from the L–G scheme (Table IX). The L–G theory and the W–F theory are again shown to be comparable in the description of the excimer formation process.

## VI. Conclusions

The L–G approach to the kinetic description of excimer formation and dissociation involving end groups of a polymer chain has been compared to the Birks scheme. Detailed analysis showed that the Birks scheme holds only if the overall deactivation rate for excited monomer and excimer is slower than the internal relaxation rate of the polymer chain.

The significance of rate constants $k_1$ and $k_{-1}$ is discussed in terms of both the W–F theory and the L–G theory. The effect of each of the parameters necessary to describe the kinetics in terms of the L–G theory on the magnitudes of $k_1$ and $k_{-1}$ is examined.

Lastly, the kinetic data of Winnik et al. have been treated in terms of the L–G model. The treatment led to the knowledge of $D$, the coefficient of relative diffusion between polymer chain ends. The values of $D$ obtained were found to be in good agreement with those calculated from using eq 9 of the W–F theory.

**Acknowledgment.** The author thanks NSERC Canada and the Department of Chemistry at the University of Calgary for financial support of this work.

## References and Notes


(1) (a) Winnik, M. A.; Redpath, A. E. C.; Panton, K.; Danhelka, J. *Polymer* **1984**, *25*, 91. (b) Winnik, M. A. In *Molecular Dynamics in Restricted Geometries*; Klafter, J., Drake, J. M., Eds.; Wiley: New York, 1989.
(2) Birks, J. B. *Photophysics of Aromatic Molecules*; Wiley-Interscience: New York, 1970.
(3) Wilemski, G.; Fixman, M. *J. Chem. Phys.* **1973**, *58*, 4009.
(4) Wilemski, G.; Fixman, M. *J. Chem. Phys.* **1974**, *60*, 866.
(5) Wilemski, G.; Fixman, M. *J. Chem. Phys.* **1974**, *60*, 878.
(6) Doi, M.; Edwards, S. F. *The Theory of Polymer Dynamics*; Clarendon Press: Oxford, 1986.
(7) Doi, M. *Chem. Phys.* **1975**, *9*, 455.
(8) Sunagawa, S.; Doi, M. *Polym. J.* **1975**, *7*, 604.
(9) Sunagawa, S.; Doi, M. *Polym. J.* **1975**, *8*, 239.
(10) Weixelbaumer, W. D.; Bürbaumer, J.; Kauffman, H. F. *J. Chem. Phys.* **1985**, *83*, 1980.
(11) Hauser, M.; Frey, R.; Klein, U. K. A.; Gosele, U. *Acta Phys. Chem.* **1977**, *23*, 21.
(12) Sienicki, K.; Winnik, M. A. *J. Chem. Phys.* **1987**, *87*, 2766.
(13) Liu, G. J.; Guillet, J. E. *Macromolecules* **1990**, *23*, 4292.
(14) De Gennes, P.-G. *Scaling Concepts in Polymer Physics*; Cornell University Press: Ithaca, NY, 1979.
(15) Chandrasekhar, S. *Rev. Mod. Phys.* **1943**, *15*, 1.
(16) Liu, G. J.; Guillet, J. E. *Macromolecules* **1990**, *23*, 2969.
(17) Bueche, F. *Physical Properties of Polymers*; Interscience: New York, 1962.
(18) Rice, A. S. In *Comprehensive Chemical Kinetics*; Banford, C. H., Tripper, C. F. H., Compton, R. G., Eds.; Elsevier: New York, 1985.
(19) Brandrup, J.; Immergut, E. H. *Polymer Handbook*, 3rd ed.; Wiley: New York, 1989.
(20) Birks, J. B.; Kazzaz, A. A. *Proc. R. Soc. London* **1968**, *A304*, 291.
(21) Lennard-Jones, J. E.; Devonshire, A. F. *Proc. R. Soc. London* **1937**, *A163*, 53.
(22) Warshel, A.; Huler, E. *Chem. Phys.* **1976**, *6*, 4631.
(23) Mahanty, J.; Ninham, B. W. *Dispersion Forces*; Academic Press: London, 1976.
(24) Kirkwood, J. G.; Riseman, J. *J. Chem. Phys.* **1948**, *16*, 565; **1954**, *22*, 626.
(25) Mandelkern, L.; Flory, P. J. *J. Chem. Phys.* **1952**, *20*, 211.
(26) Liu, G.; Guillet, J. E.; Al-Takrity, E. T. B.; Jenkins, A. D.; Walton, D. R. M. *Macromolecules* **1990**, *23*, 4164.
(27) Anufrieva, E. V.; Gotlib, Yu. Ya. *Adv. Polym. Sci.* **1981**, *40*, 1.
(28) Martinho, J. M. G.; Winnik, M. A. *J. Phys. Chem.* **1987**, *91*, 3640.


**Registry No.** Pyrene, 129-00-0.